Localized plasmons in nanostructures

Eduardo Arqué López
*Facultat de Física, Universitat de Barcelona, Diagonal 645, 08028 Barcelona, Spain.**

Advisor: Dr. Xavier Batlle
Department of Condensed Matter Physics

Abstract: Plasmon resonances in nanospheres, nanoshells and nanorods are discussed through the study of the optical extinction spectra. The formation of dipolar electric fields and charge density distributions for small nanoparticles is observed, thus confirming the validity of the quasistatic approximation of Mie theory, which is found to hold up to particle sizes of about 150 nm. Finally, plasmon coupling effects are studied in nanorod dimers where huge electric field enhancement is observed.

I. INTRODUCTION

Plasmonics is the field that studies the interaction between electromagnetic radiation and the conduction electrons, *i.e.* the plasmons, in small metal particles, usually of sizes in the nanometric scale. The field is divided in two main manifestations of the plasmonic effects: surface plasmon polaritons and localized surface plasmons, the latter being the object of this study.
Localized surface plasmons are non-propagating excitations of the electron cloud in the metal caused by an external electromagnetic field. This field exerts a force on the electron cloud, polarizing it. The polarization is maximum at a certain position in the spectrum, the localized surface plasmon resonance (LSPR) [1]. Plasmon resonances modify the optical properties of the material and a number of applications have been found for very different fields like biomedicine or nanophotonics [2], [3], [4].
In this work we study plasmonic effects using simulation methods on several gold nanoparticles: nanospheres, nanoshells and nanorods. The election of gold as the nanostructure material was motivated by the fact that resonances fall in the visible spectrum [1], and because it is widely used in applied research due to its plasmonic response and biocompatibility [5].

II. THEORETICAL BACKGROUND

The condition for plasmonic resonance can be obtained analytically for various simple structures, such as the ones treated in this work. This is done by solving the problem of an electromagnetic wave being scattered by a small metal particle. This problem was studied in 1908 by the German physicist Gustav Mie [6], where he analized from an electrodynamic point of view, using multipole expansions, the scattering of radiation by small gold spheres. When the particle size is significantly smaller than the light wavelength, the *quasistatic* approximation can be applied. All multipole orders higher than the dipole are neglected, which simplifies enormously the analytic treatment of the problem. Spatial variations of the incoming electric field are also neglected, so the problem is reduced to electrostatics: solving the Laplace equation for the electric potential $\nabla^2\Phi = 0$, and then finding the electric field $\mathbf{E} = -\nabla\Phi$. Considering a gold nanosphere of radius R, dielectric function $\varepsilon(\omega)$; surrounded by a medium with dielectric constant ε_m, and an incident electric field $\mathbf{E} = E_0\hat{\mathbf{z}}$, and solving the Laplace equation in spherical coordinates with the proper boundary conditions leads to [7]:

$$\Phi_{in} = -\frac{3\varepsilon_m}{\varepsilon(\omega)+2\varepsilon_m}E_0 r\cos\theta \tag{1a}$$

$$\Phi_{out} = -E_0 r\cos\theta + \frac{\varepsilon(\omega)-\varepsilon_m}{\varepsilon(\omega)+2\varepsilon_m}E_0 R^3\frac{\cos\theta}{r^2} \tag{1b}$$

which are the potentials inside (Φ_{in}) and outside (Φ_{out}) the sphere. Equation (1b) can be rewritten in terms of a dipole moment $\mathbf{p}$:

$$\Phi_{out} = -E_0 r\cos\theta + \frac{\mathbf{p}\cdot\mathbf{r}}{4\pi\varepsilon_0\varepsilon_m r^3} \tag{2a}$$

$$\mathbf{p} = 4\pi\varepsilon_0\varepsilon_m R^3\frac{\varepsilon(\omega)-\varepsilon_m}{\varepsilon(\omega)+2\varepsilon_m}\mathbf{E_0} \tag{2b}$$

Φ_{out} is composed of a superposition of the applied field and a dipole $\mathbf{p}$ in the centre of the sphere, showing that the external field induces the electric dipole.
Having obtained this induced dipole moment, the polarizability α is introduced:

$$\alpha = 4\pi R^3\frac{\varepsilon(\omega)-\varepsilon_m}{\varepsilon(\omega)+2\varepsilon_m} \tag{3}$$

defined by $\mathbf{p} = \varepsilon_0\varepsilon_m\alpha\mathbf{E_0}$, and is in principle a complex quantity. The polarizability is an important quantity for plasmonic effects, because it describes the tendency of a charge distribution to have its charges displaced by an external field. Minimizing the denominator in equation (3) provides a condition for the resonant enhancement of α, the Frölich condition:

$$\mathbf{min}|\varepsilon(\omega)+2\varepsilon_m| \tag{4}$$

*Electronic address: earquelo10@alumnes.ub.edu

The dielectric function $\varepsilon(\omega)$ can be separated in its real and imaginary parts:

$$\varepsilon(\omega) = \varepsilon_1(\omega) + i\varepsilon_2(\omega) = n^2 - \kappa^2 + i(2n\kappa) \tag{5}$$

where n is the refractive index of the material and κ is the extinction coefficient. The latter is related to the absorption coefficient of the material, which quantifies the absorption of light by the medium [8]. With the dielectric function expressed as eq. (5), the Frölich condition simplifies to $\varepsilon_1 = -2\varepsilon_m$, since ε_2 varies slowly over the visible spectrum in gold [9]. Another important quantity derived from α is the extinction cross section σ_{ext}, which is the sum of the scattering and absorption cross sections, and is defined as the absorbed and scattered power divided by the incoming flux power [7]:

$$\sigma_{ext} = \sigma_{abs} + \sigma_{sca} = k\mathrm{Im}[\alpha] + \frac{k^4}{6\pi}|\alpha|^2 \tag{6}$$

If instead of a nanosphere, the object is a nanoshell, which is a dielectric sphere of radius a_i and dielectric function $\varepsilon_i(\omega)$ coated with a gold thin layer of radius a_e and dielectric function $\varepsilon(\omega)$, the quasistatic polarizability is [1]:

$$\alpha = 4\pi a_e^3 \frac{(\varepsilon - \varepsilon_m)(\varepsilon_i + 2\varepsilon) + f(\varepsilon_i - \varepsilon)(\varepsilon_m + 2\varepsilon)}{(\varepsilon + 2\varepsilon_m)(\varepsilon_i + 2\varepsilon_m) + f(2\varepsilon - 2\varepsilon_m)(\varepsilon_i - \varepsilon)} \tag{7}$$

where $f = a_i^3/a_e^3$ is the volume fraction ocuppied by the inner sphere.

The geometry of a nanorod, a cylindrical shaped solid gold structure, is difficult to treat analytically, but the quasistatic plasmon resonance condition is well reproduced by approximating the nanorod by a prolate spheroid, an ellipsoid of principal axes $a > b = c$. Under this approximation, the polarizability along a given axis ($i = x, y, z$) is [1]:

$$\alpha_i = \frac{4\pi abc(\varepsilon(\omega) - \varepsilon_m)}{3\varepsilon_m + 3L_i(\varepsilon(\omega) - \varepsilon_m)} \tag{8}$$

where L_i is the depolarization factor of the i axis, which is, considering that a is the length in the x direction:

$$L_x = \frac{1 - e^2}{e^2}\left(-1 + \frac{1}{2e}\ln\frac{1+e}{1-e}\right) \tag{9a}$$

for the longest axis,

$$L_y = L_z = \frac{1 - L_x}{2} \tag{9b}$$

for the other two, where $e^2 = 1 - \left(\frac{b}{a}\right)^2$ is the ellipticity of the ellipsoid.

Finally, when two nanostructures that show plasmonic effects are placed closely, plasmon coupling through the near-field arises: plasmon resonances of the nanoparticles interact with each other giving rise to coupled plasmon modes. These modes depend on the relative alignment of the nanoparticles and the polarization of the light source. A hybridization model, as an electrodynamic analogy to the molecular orbital hybridization, has been proposed to explain the behaviour observed in different nanoparticle plasmon coupling [10], for example in dimers, *i.e.* pairs of similar nanostructures, or nanoshells.

III. SIMULATION METHOD

All of the results presented in this work were obtained with *Lumerical FDTD solutions* [11]. The program solves Maxwell's equations with boundary conditions using the finite difference time domain (FDTD) method, a computational method proposed by Kane Yee in 1966 [12], where partial differential equations are discretized to finite difference equations and boundary problems that were untreatable from the analytical point of view of partial differential equations become solvable. It works in time domain, contrary to methods working in frequency or Fourier domain. All simulations were carried out in vacuum ($\varepsilon_m = 1$), using the gold dielectric function data of Johnson and Christy [13], and a plane wave excitation source inciding normally on the nanostructure.

IV. RESULTS AND DISCUSSION

A. Nanosphere

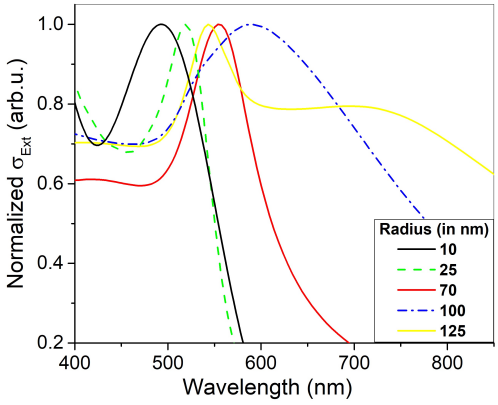

FIG. 1: Normalized σ_{ext} of nanospheres with different sizes.

FIG. 1 shows σ_{Ext} spectrum for nanospheres with different sizes. A common trend is found in all sizes studied: at $\lambda = 400$ nm, σ_{ext} is relatively high, then decreases slightly below 450 nm, increases again reaching a maximum and finally decreases more or less sharply.

The first region of the spectrum is characterized by electronic interband transitions, where absorption increases because photons of $\lambda < 450$ nm cause electronic interband transitions. A huge enhancement of σ_{ext} is seen

in the second region, for wavelengths $450 < \lambda < 650$ nm depending on the nanosphere size. The peak in this region is the LSPR peak, where α is greatly enhanced. For longer wavelengths after the resonance condition has been met, the decrease of both α and the wavevector $k = 2\pi/\lambda$ cause the decrease of σ_{ext} (eq. (6)).
The $R = 25$ nm curve is the perfect example of the validity of the quasistatic approximation: a narrow resonance peak described by the Frölich condition (eq. (4)), which induces an electric dipole inside the sphere, causing a dipolar electric field and charge density distribution. FIG. 2 shows electric field and charge density distribution of two different nanospheres. The dipolar nature of a plasmonic resonance in the quasistatic regime can be observed in the **E** field and charge distribution (FIG. 2 **(a), (c)**) obtained for the λ at the maximum of the green dashed line in FIG. 1, corresponding to the $R = 25$ nm nanosphere.
Increasing the nanosphere radius causes a redshift and a broadening of the peak, as seen in the $R = 70$ nm and $R = 100$ nm curves of FIG. 1. This is explained by retardation effects. The quasistatic approximation considers a static electric field, but when the quasistatic condition, *i.e.* $R << \lambda$, is not completely satisfied, spatial variations of the incoming electric field appear over the nanosphere volume. These effects become very large for $R = 125$ nm where the σ_{ext} spectrum is significantly different from the rest of the cases. A peak is found at shorter wavelengths than the $R = 100$ nm peak, and a very slow decrease of σ_{ext} is observed. This indicates that the quasistatic approximation does not hold for nanospheres of radii $R \geqslant 100$ nm, and therefore higher order multipole modes have to be considered. Thus, the extinction spectrum of the $R = 125$ nm nanosphere can be explained taking into account contributions of a dipole mode, which follows the redshifting and broadening trend of the other nanospheres, and a quadrupole mode that causes a resonance peak at shorter wavelengths than the dipole one. FIG. 2 **(b)** and **(d)** show the quadrupole mode in a $R = 125$ nm nanosphere. These electrodynamic effects that arise because electric fields are no longer static are called *extrinsic size effects* [14],[15]. Finally, the $R = 10$ nm curve also deviates from the quasistatic regime behaviour of $R = 25$ nm: the peak is found at shorter wavelengths and also broadened. These effects arise because the nanosphere size is inferior to the electron mean free path in Au ($l \sim 30$ nm) [15], and surface scattering of electrons is no longer negligible. This is accounted for by introducing a size dependent dielectric function $\varepsilon(\omega) \to \varepsilon(\omega, R)$ [14]. These latter effects caused by the sphere size but that do not depend on external fields, are called *intrinsic size effects*.

B. Nanoshell

The polarizability of nanoshells (eq. (7)), shows that the ratio f plays an important role determining the position of the resonance peak. Therefore, nanoshells present a huge tunability of the position of the LSPR peak over the spectrum given the fast variation of f with different radii because of the cubic exponent. FIG. 3 shows the extinction cross section of nanoshells with different internal and external radii. The great tunability is clearly seen: dipole peak positions shift from $\lambda = 557$ nm to $\lambda \approx 700$ nm increasing the ratio f. Nanoshells present more intense peaks than nanospheres, and therefore a superior polarizability and electric field enhancement, as shown in FIG. 4 **(a)** where the electric field intensity, calculated for the maximum in FIG. 3, is higher than the nanosphere case (FIG. 2 **(a)**). We observe a dipolar distribution for both electric field and charge distributions in a $a_e = 21$ nm nanoshell (FIG. 4 **(a), (c)**), which confirms the validity of the quasistatic approximation. **E** also decreases faster with distance, so the field is more localized. Charge accumulates at both surfaces of the shell, external and internal, as expected for a conductor like gold.

Extrinsic size effects are also observed in nanoshells.

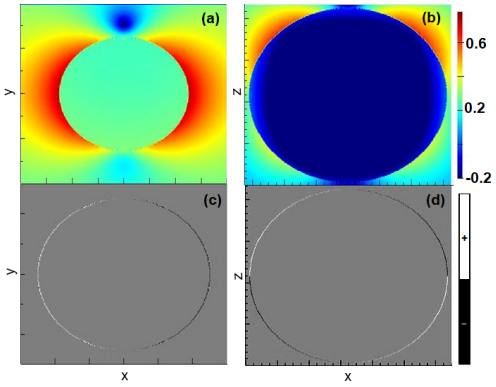

FIG. 2: Electric field (log scale) [**(a),(b)**] and charge density distribution [**(c),(d)**] of **(a), (c)** $R = 25$ nm nanosphere for $\lambda = 520$ nm; **(b), (d)** $R = 125$ nm nanosphere for $\lambda = 543$ nm

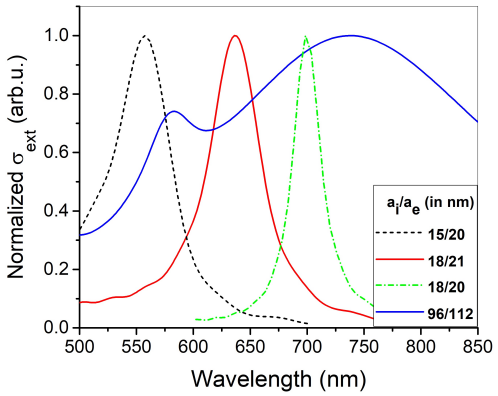

FIG. 3: Normalized σ_{ext} of nanoshells with different a_i and a_e. Red and blue solid lines correspond to nanoshells with equal $f = (6/7)^3$.

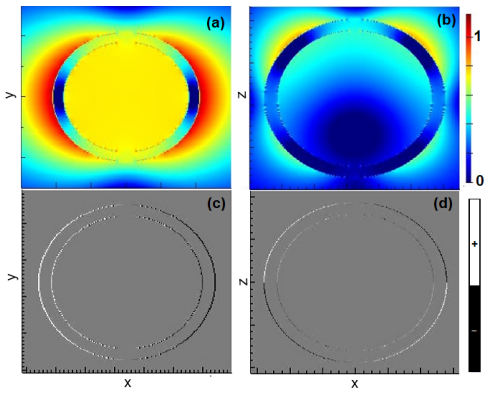

FIG. 4: Electric field (log scale) [**(a),(b)**] and charge density distribution [**(c),(d)**] of nanoshells with the same ratio $f = (6/7)^3$. **(a), (c)** $a_i = 18$ nm, $a_e = 21$ nm for $\lambda = 636$ nm; **(b), (d)** $a_i = 96$ nm, $a_e = 112$ nm for $\lambda = 582$ nm.

σ_{ext} of two nanoshells with the same ratio f show different peak positions. Increasing both internal and external radius, while keeping the same ratio f, causes the LSPR peak to redshift and broaden, the same effects observed in FIG. 1 for nanospheres. We also note the appearance of a quadrupole peak in the $a_e = 112$ nm curve around $\lambda \approx 575$ nm, which is still less intense than the dipole peak at $\lambda \approx 750$ nm. Quadrupolar field and charge density distributions are seen for the $a_e = 112$ nm case in FIG. 4 **(b), (d)** respectively, where quasistatic conditions do not apply because of the nanoshell size. Since the height of the quadrupole peak in σ_{ext} is lower than the dipole peak, a reduced electric field intensity and charge density are expected. Comparing FIG. 4 **(b)** with **(a)** and **(d)** with **(c)** we observe that this is the case.

C. Nanorod

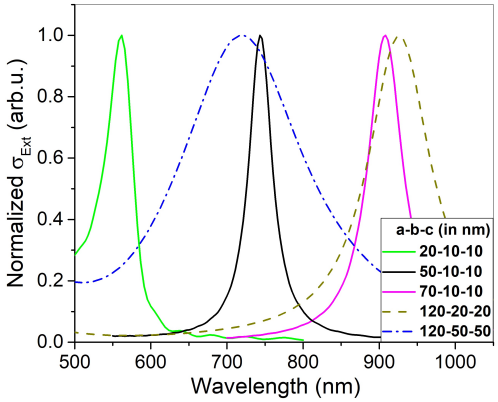

FIG. 5: Normalized σ_{ext} of nanorods with different sizes.

The σ_{ext} of nanorods with different sizes for an incoming field polarized in the direction of the long axis a is shown in FIG. 5. We observe that the resonance peak can be tuned by varying the different nanorod lengths a, b and c. This result is expected from the polarizability expression of a nanorod in the quasistatic approximation (eq. (8)), where the depolarization factor L_i that depends on the ellipticity e and thus, on the nanorod size, controls the resonance peak position. The peak position is displaced from $\lambda \approx 550$ nm to $\lambda > 900$ nm by varying the lengths a, b, c, and redshifting is stronger for e closer to unity, *i.e.* when the ratio b/a is smaller.
Electric field and charge density distribution of a $a = 50$, $b = c = 10$ nm are shown in FIG. 6 **(a)** and **(b)** respectively. We observe that the electric field intensity is larger than in the $a_e = 21$ nm nanoshell, due to the sharper enhancement of α. Another interesting feature of nanorods is that the quasistatic regime holds for bigger sizes if only one of the lengths is enlarged. For a nanorod with dimensions $a, b, c = 120, 20, 20$ nm respectively, the peak is strongly redshifted, but the peak width is still comparable to those of smaller sizes. However, the peak is slightly more redshifted than the $a, b, c = 70, 10, 10$ nm curve, even though e is closer to 1 in the latter. When the b and c lengths are enlarged, the peak shows a large broadening and a blueshift due to e being smaller. There is no sign of a quadrupole peak in the $a, b, c = 120, 20, 20$ nm spectrum, but the slightly higher extinction outside the peak region indicates a deviation from the quasistatic regime which can be explained by a small contribution to the extinction by a quadrupolar mode.

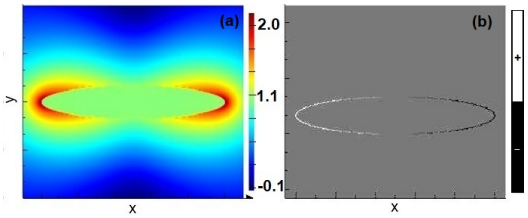

FIG. 6: Electric field (log scale) [**(a)**] and charge density distribution [**(b)**] of a nanorod with sizes $a = 50$ nm, $b = c = 10$ nm, for $\lambda = 744$ nm.

D. Nanorod dimers

FIG. 7 shows σ_{ext} of nanorod dimers in longitudinal and transverse alignment, relative to the incoming electric field polarization. When nanorods are separated 100 nm in longitudinal alignment, the LSPR peak wavelength coincides with the single nanorod case, at $\lambda = 750$ nm (green dashed line in FIG. 7 and black solid line in FIG. 5). As separation is reduced, a redshifting of the peak from $\lambda = 750$ nm to $\lambda = 782$ nm is observed. This behaviour is explained by the hybridization model, since two nanorods aligned longitudinally can form a hybridized bond reducing the energy [10],

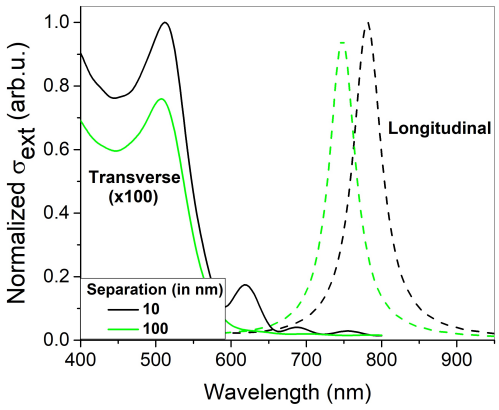

FIG. 7: Normalized σ_{ext} of nanorod dimers of sizes $a = 50$ nm, $b = c = 10$ nm 10 nm and 100 nm separation; for longitudinal modes (dashed curves) and transverse modes. The transverse mode σ_{ext} has been multiplied by a factor 100 in order to compare with the longitudinal mode.

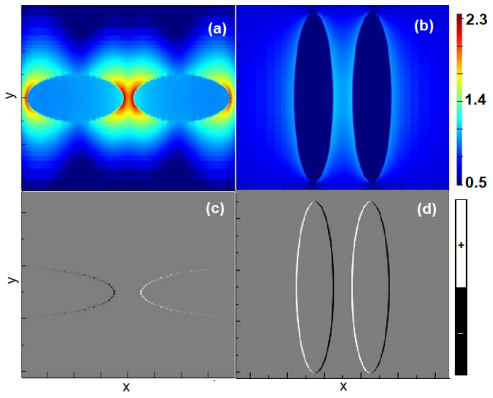

FIG. 8: Electric field (log scale) [**(a),(b)**] and charge density distribution [**(c),(d)**] of nanorod dimers with sizes $a = 50$ nm, $b = c = 10$ nm. **(a),(c)** Longitudinal alignment at $\lambda = 782$ nm; **(b),(d)** Transverse alignment at $\lambda = 512$ nm.

thus redshifting the peak position. The transverse mode (black solid line in FIG. 7) shows a plasmon resonance peak at $\lambda = 512$ nm for a 10 nm separation. The peak is slightly blueshifted for 100 nm separation (green solid line), and located at $\lambda = 507$ nm. This behaviour is also explained by the hybridization model [10].
For longitudinal modes, the plasmon coupling produces a huge enhancement of the electric field in the region between the nanorods (FIG. 8 **(a)**), whereas the field enhancement in the transverse case is inferior by two orders of magnitude (FIG. 8 **(b)**), which is expected from the peak intensity differences in the extinction spectrum. Charge density distributions (FIG. 8 **(c), (d)**)) are both dipolar, consistent with the limit of the quasistatic regime for nanorods and the charge distribution of a single nanorod shown in FIG. 6 **(b)**.

V. CONCLUSIONS

FDTD simulations have been performed for nanospheres, nanoshells and nanorods, finding plasmon resonance effects in the optical extinction spectrum peaks. Plasmon resonances cause dipolar field and charge density distributions in the quasistatic regime, valid for sizes below 150 nm, and quadrupolar distributions in bigger structures; as well as electric field enhancement. The great tunability in plasmonic response of nanoshells and nanorods, due to the effect of the aspect ratio in the polarizability, has also been confirmed. Finally, plasmonic coupling effects in nanorod dimers have been found to produce very strong electric field enhancement in the near field.

Acknowledgments

This work was supported by Spanish MINECO (MAT2015-68772-P,) and the European Union FEDER funds. I want to thank my advisor Prof. Xavier Batlle and Dr. Ana Conde for their continuous help and guidance throughout the process of this work. I also want to thank my parents for their invaluable support.

[1] S.A. Maier, *Plasmonics: fundamentals and applications*, (Springer US, 2007, 1st. ed.)
[2] G. Baffou and R. Quidant, Laser & Photonics Reviews, 7: 171-187 (2013).
[3] H. Heidarzadeh *et al.*, Appl. Opt. 55, 1779-1785 (2016)
[4] J. Anker *et al.* Nature Materials vol. 7, 442-453 (2008).
[5] T. A. Erickson and J. W.Tunnell, in Nanotechnologies for the Life Sciences, C. S. Kumar (Ed.) (2010).
[6] G. Mie, Ann. Phys., 330: 377-445, (1908).
[7] J.D Jackson, *Classical Electrodynamics*, (John-Wiley & Sons, New York 1975, 2nd. ed.)
[8] M. Fox, *Optical Properties of Solids* (Oxford University press, Oxford 2010, 2nd. ed.)
[9] Robert L. Olmon *et al.* Phys. Rev. B 86, 235147, (2012).
[10] P. K. Jain *et al.*, J. Phys. Chem. B, (2006), 110, 18243.
[11] https://www.lumerical.com/tcad-products/fdtd/
[12] K. Yee, IEEE Transactions on Antennas and Propagation, vol. 14, no. 3, pp. 302-307, (1966).
[13] P. B. Johnson and R. W. Christy, Phys. Rev. B 6, 4370, (1972).
[14] U. Kreibig & M. Vollmer, *Optical properties of metal clusters*, (Springer Verlag, Berlin Heidelberg 1995, 1st. ed.)
[15] V. Amendola *et al.* J. Phys.: Condens. Matter 29 203002, (2017).